

The Creep Behavior of Solid-Filled Rubber Composites

Chao-Hsun Chen* and Yih-Cheng Chen

Institute of Applied Mechanics National Taiwan University, Taipei 10764, Taiwan, R.O.C

(Received February 10, 1993; Accepted August 31, 1993)

Abstract: This paper is using an experimental method to study the creep behavior of solid-filled silicone-rubber composites (GFSC). The specimens made of silicone-rubber as the matrix and 0~40% volume fraction (V_f) of glassbeads, have been through uniaxial tensile tests and constant-loading creep tests. The results show that the material behavior is obviously nonlinear and the Eyring's reaction rate principle is suitable to describe the viscoelastic behavior of this rubber composite. Thus, to solve the creep problems of rubber composites, the Boltzmann's superposition technique can not be applied. Although Findley et. al (1976), have proposed the multiple integrals form, but solving the multiple integrals form is quite complicated and does not guarantee convergence. We have employed So-Chen's form of the nonlinear stress-strain relationship of rubber elasticity. This can avoid the above mentioned problems and the analytic solution is obtained. The resulting solution is in very good agreement with the experimental results.

Keywords: Creep, Particle-reinforced, Rubber composite, Nonlinear four-element Burger's model.

Introduction

Recently, composites have been more widely used due to its merits of increasing material toughness, strength, impact resistance, propelling power, etc.; properties that are more suitable for engineering applications. Solid propellant is a high volume fraction of solid-filled rubber composites. The rubber matrix itself exhibits viscoelastic behavior. Therefore, the stress and strain are a function of time. The main theme of this paper is to study the viscoelastic behavior of the solid-filled rubber composites, by employing the glass beads-filled silicone rubber composites of the solid-filled silicone-rubber composites (GFSC) to simulate the viscoelastic behavior of this type of composites. We have employed the So-Chen's NFEB model for the GFSC, which describes the nonlinear stress-strain relation of rubber elasticity. This nonlinear model will be subject to uniaxial tensile test, creep test, and stress-relaxation test.

For linear viscoelastic material there is complete description, in continuum mechanics literature [1], [2] and [3]. For the stress-strain and time integral representation, the simplest way is employing the Boltzmann's superposition method, where the time-

function relation between compliance and relaxation modulus refers to the mechanical response as being related to the loading history, then the effects of these small time intervals are superimposed to form the integral representation. The differential representation of the stress-strain as being related to time is done by superimposing the linear spring and Newton dashpot to form the mechanical model, for example, Maxwell model, Kelvin model, Four-element Burger's model, generalized Maxwell model, ... etc., in order to analyze the mechanical behavior under the differential time, the stress or strain. This representation form is popularly adopted in experiments because the material constants determined from the creep experiments can well describe the material mechanical behavior.

For nonlinear viscoelastic material, even under very small strain conditions the stress-strain relationship is still nonlinear. The Boltzmann's superposition method can no longer be applied. To extend this method, Findley et al. [5] directly expanded the nonlinear integral to multiple integral representation form and Rivlin derived from the had relation of materials with memory. The employment of the continuum mechanics method [6] and [7] encountered the difficulty of convergence of the multiple integrals. Schapery

* To whom all correspondence should be addressed.

[8] who employed thermodynamics, derived a simple integral form by adding a nonlinear modified term to describe the nonlinear stress-strain relationship, and successfully reduced it back to a linear relation. Furthermore, we can find suitable nonlinear elements (similar to So-Chen's [12]) to form the nonlinear mechanical model which can well describe the nonlinear mechanical behavior. We treated each individual molecular chain as the "entropy spring" and employed the rubber elasticity formula to replace the linear spring. Also, from the concept of nonlinear activation energy jump over the energy barrier, we employed the Eyring activation energy dashpot to replace the Neeson's dashpot.

Experiment

The specimens used in the uniaxial tensile creep tests were made by using the silicone rubber as the matrix, with the glassbeads from 0~40 percent of V_f and T40913 hardener (from Wacker-Chemic GmbH). Their individual properties are as follows:
 Silicone rubber:(RTV-M457 from Wacker-Chemic GmbH)

- Stiffness:40 (shore A)
- density:1.24 (g/cm³)
- Poisson ration (ν): 0.499
- Young's modulus (E): 1.08 (MPa)
- Shear modulus (G): 0.363 (MPa)

Glassbeads: (from Toshiba-Ballotini company, Japan)

- Diameters: 105~210 μ m
- Poisson ratio (ν): 0.24
- Young's modulus (E): 68500 (MPa)
- Shear modulus (G): 27600 (MPa)

Tensile specimens of gage lengths of 20 mm in accordance with ASTM D412 were cut from sheets. All specimens were kept in a desiccator for 15 days for post curing and to stabilize their properties. They were then used in creep tests under constant loads. All the tensile tests and creep tests were performed in a laboratory environment of 50% relative humidity (RH) at 25°C.

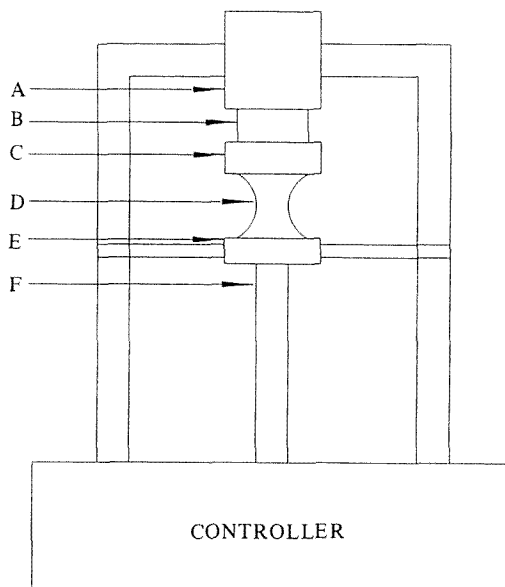
Mechanical behavior and model analysis

As the polymer matrix itself is very much strain rate and time dependent, the studies of the influence for different volume fraction of inhomogeneities on

its tensile strength, creep behavior and stress relaxation behavior become very important. In this section, what follows is the rubber elasticity and the Eyring's reaction rate principle derived from the micro-molecular-chain's deformation under stresses. The molecular jumping velocities between two energy steps are recapitulated first, then applied to construct the NFEB model.

1. Stress-strain relation

From the table type loading machine (Figure 1), four strain rate of 0.01, 0.02, 0.06 and 0.1 (1/sec) tests were conducted. Figures 2~4 show that within these strain rate ranges, the stress-strain relation makes not much difference. Besides, the smaller strain rate the specimen undergoes, the shorter elongation the specimen can take before it fractures. The tensile strength and the elongation increase as the strain rate increase. The stress-strain curves show that even under very small strain condition, this material still exhibits very strong nonlinear relation, therefore, the linear mechanical model cannot be applied to describe the mechanical behavior of this material. The Engineering stress σ and engineering strain ϵ are defined as follows:



- A. Fixed Plate
- B. Load Cell
- C. Upper Grip
- D. Specimen
- E. Lower Grip
- F. Transmission Axis

Figure 1. Table-type loading machine

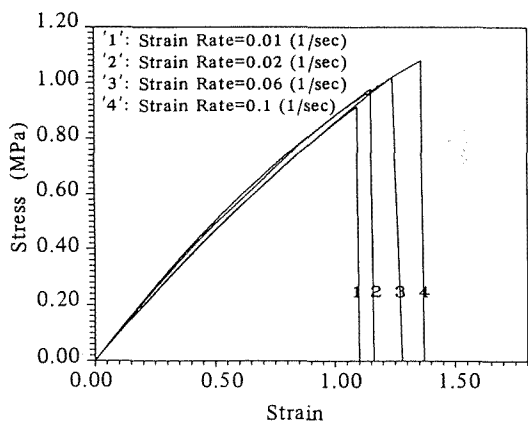


Figure 2. Rate dependence of the stress-strain curve for the pure silicone rubber matrix.

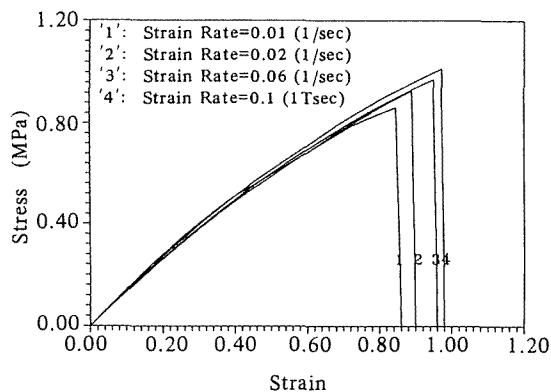


Figure 3. Rate dependence of the stress-strain curve for the 20% V_f of GFSC.

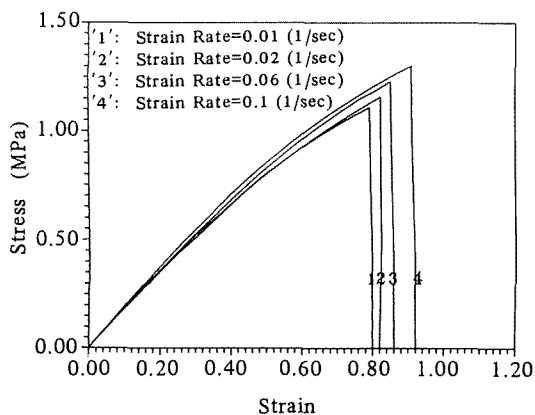


Figure 4. Rate dependence of the stress-strain curve for the 40% V_f of GFSC.

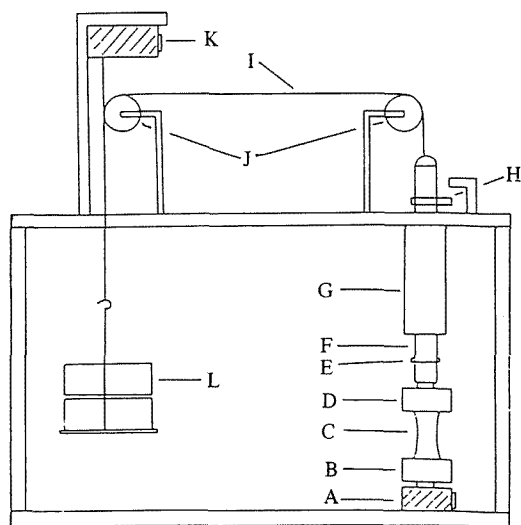
$$\sigma = \frac{P}{A_0} \tag{1}$$

$$\epsilon = \frac{L - L_0}{L_0} \tag{2}$$

Where A_0 is the original cross-section area, L and L_0 are the length before and after deformation respectively, and P is the applied force on the specimen.

2. Creep behavior

The creep loading machine (Figure 5) is used to determine the creep strain-time relation under constant loading. From Figures 6-9, it shows that the difference between GFSC and the pure silicone-rubber is that GFSC shows interface bonding properties. Since the bonding force between the glassbeads and the silicone-rubber matrix are not strong enough, the more the filled glassbeads, the more debonding behavior along the interfaces occurs. Thus the strain rate of the steady-state stage increases with increas-



- A. Load Cell
- B. Lower Grip
- C. Specimen
- D. Upper Grip
- E. SA top Block (For Stress-Relaxation Test)
- F. Slide Pole
- G. Cover
- H. Stop Block (For Specimen)
- I. Steel Wire
- J. Slide Wheel
- K. Displacement Transformer
- L. Weight

Figure 5. Creep testing machine.

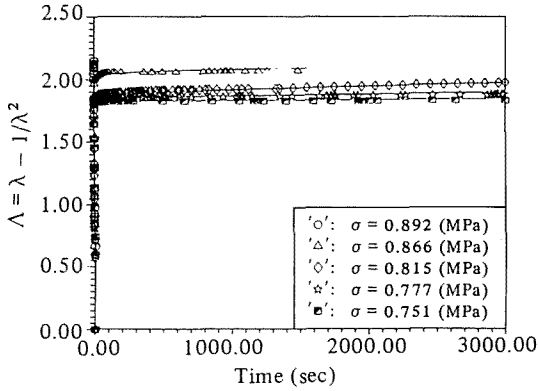


Figure 6. Stress dependence of the creep strain Λ for the 10% V_f of GFSC, where the solid line is the NGE model's calculation and the mathematical index is the experimental results.

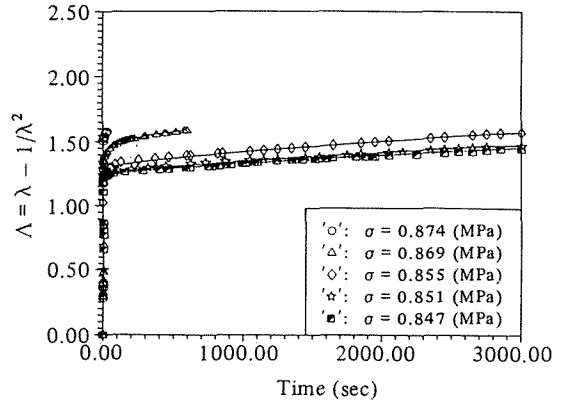


Figure 9. Stress dependence of the creep strain Λ for the 40% V_f of GFSC, where the solid line is the NGE model's calculation and the mathematical index is the experimental results.

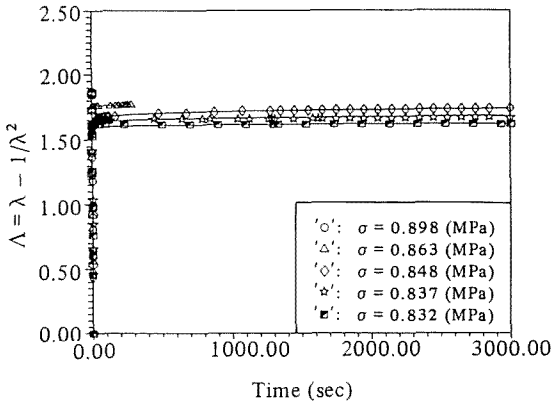


Figure 7. Stress dependence of the creep strain Λ for the 20% V_f of GFSC, where the solid line is the NGE model's calculation and the mathematical index is the experimental results.

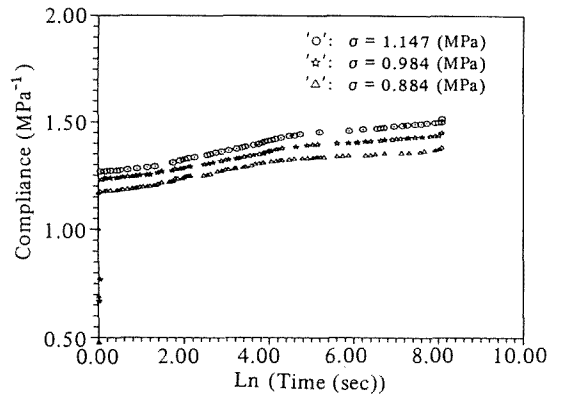


Figure 10. Stress dependence of the creep compliance $C(t) = \epsilon(t) / \sigma$ for the pure silicone rubber.

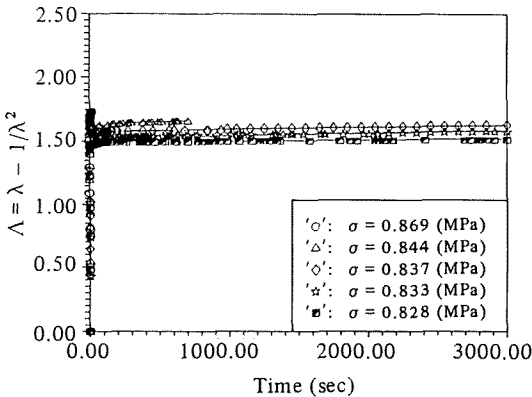


Figure 8. Stress dependence of the creep strain Λ for the 30% V_f of GFSC, where the solid line is the NGE model's calculation and the mathematical index is the experimental results.

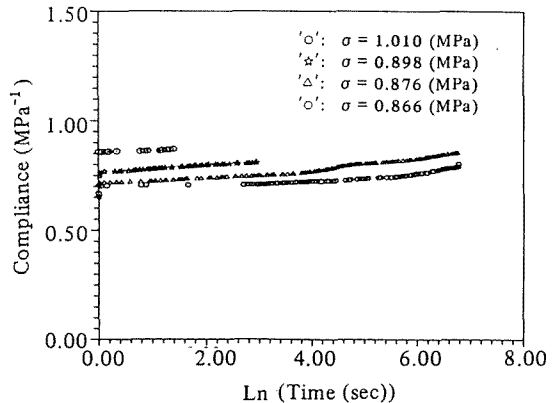


Figure 11. Stress dependence of the creep compliance $C(t) = \epsilon(t) / \sigma$ for the 40% V_f of GFSC.

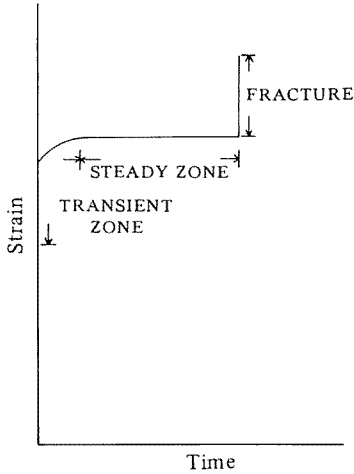


Figure 12. Creep history diagram.

ing V_f of glassbead (ie. the viscous flow is more evident) Also, the coefficient of the creep compliance relation $C(t) = \epsilon(t) / \sigma$ (in Figures 10~11) shows that the $C(t)$ increases with increasing stress, and their relation is obviously nonlinear.

Form Figure 12 we can distinguish the creep history into three stages, which are

- a. Transient stage: After the initial stretch, the slippage of the molecular chain changes from very obvious to steady state. Therefore, the strain rate that started from the maximum value would reduce to a constant value. Here we call this started as the first stage of the creep.
- b. Steady Stage: When the slippage of the molecular chain reaches the steady state, the whole molecular structure also reaches the thermodynamic equilibrium, at which the strain rate is almost a constant. Here we call this stage as the second stage of the creep.
- c. Fracture stage: In this stage the material fractures with no symptoms in advance.

3. Nonlinear four-element burger's model

The above uniaxial tensile test and creep test results show that the material behavior is nonlinear, therefore, we have adopted the So-Chen's NFEB model [12] to describe the mechanical behavior as follows:

Elements:

(a) Nonlinear spring: The relation between the creep strain quantity Λ and the stress σ of the rubber elasticity

$$\sigma = G\Lambda \tag{3}$$

and

$$\Lambda = \lambda - \frac{1}{\lambda^2} ; \lambda = 1 + \epsilon \tag{4}$$

where λ is the stretch ratio and G is the shear modulus. (b) Nonlinear dashpot: When the material is under stresses, it will result in the atomic structure's slippage and breakage. Tobolsky and Eyring derived the linear reaction rate formula from the micro-molecular chain and the energy barrier points of view.

$$\dot{\epsilon} = K \text{ Sinh} (v\sigma) \tag{5}$$

By extending the above linear relation to nonlinear relation we have

$$\dot{\Lambda} = A \text{ Sinh} (v\sigma) \tag{6}$$

where K and A are related to the activation energy.

$$A = K \text{ Exp} \left\{ \frac{-\Delta H}{RT} \right\} \tag{7}$$

v is the shift quantity of the energy barrier under the stresses or the activation volume, all these three are the activation mechanism index of the micro-molecular chain. This NFEB model is shown in Figure 13.

4. Constitutive equations of the GFSC

Our theory will be developed at a constant, elevated temperature. Then when the rubber matrix is subjected to a tensile stress σ , its total strain Λ creep

$$\Lambda = \Lambda_i + \Lambda_t + \Lambda_s \tag{8}$$

where

(1) Λ_i is the initial stretch

$$\Lambda_i = \sigma / G_i \tag{9}$$

and their respective creep rate of the GFSC can be

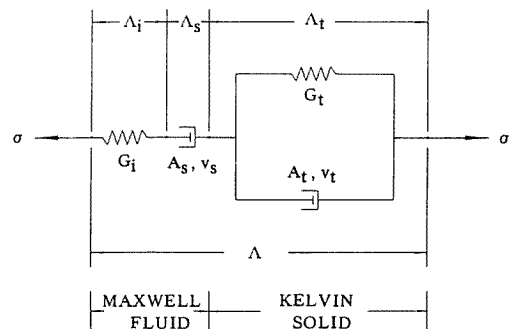


Figure13. Nonlinear Four-Element Burger's model

written as

(2) transient-stage creep rate

$$\dot{\Lambda}_t = A_t \sinh[v_t (\sigma - G_t \Lambda_t)] \quad (10)$$

By some manipulation we can rewrite $\dot{\Lambda}_t$ as

$$\dot{\Lambda}_t = \frac{2 A_t \tanh(v_t \sigma / 2) \text{Exp}(-v_t G_t A_t t)}{1 - [\tanh(v_t \sigma / 2) \text{Exp}(-v_t G_t A_t t)]^2} \quad (11)$$

where $1 > [\tanh(v_t \sigma / 2) \text{Exp}(-v_t G_t A_t t)]^2$

(3) steady-state creep rate (Eyring reaction rate for mola)

Here we assume that the time rate of change in nonlinear stretch parameter also satisfies the Eyring equation for activated non-Newtonian viscous material. Then we obtain

$$\dot{\Lambda}_t = A_s \sinh(v_s \sigma) \quad (12)$$

Therefore, the total creep strain $\Lambda(t)$

$$\Lambda(t) = \frac{\sigma}{G_t} + A_s t \text{Sinh}(v_s \sigma) + \frac{\sigma}{G_t} \left\{ 1 - \frac{2}{v_t \sigma} \text{Tanh}^{-1} \left[\text{Tanh} \left(\frac{v_t \sigma}{2} \right) \text{Exp}(-v_t G_t A_t t) \right] \right\} \quad (13)$$

where G_t, G_i, A_s, A_t, v_s and v_t are the material constants which can be determined from the creep experiments.

5. Determination of the material constants ($G_i, G_t, A_s, A_t, v_s, v_t$)

From the creep test datas, firstly, we have to transform the strain $\epsilon(t, \sigma)$ into $\Lambda(t, \sigma)$ by eq. (4), then to determine the material constants from the Λ vs time curve. Theoretically, to determine the six material constants, only two creep strain vs time curves are needed. But to determine them simultaneously there is

Table I. The material constants of the NEFB model for the different V_t of the GFSC.

V%	G_t (MPa)	A_s (1/sec)	v_t (1/MPa)	G_i (MPa)	A_t (1/sec)	v_i (1/MPa)
40	0.767	1.64E-10	20.72	2.452	1.05E-6	21.10
30	0.699	5.51E-11	22.32	2.654	9.12E-6	55.17
20	0.552	3.88E-12	24.04	3.393	1.17E-7	38.86
10	0.455	5.01E-12	25.73	8.387	2.50E-7	32.88
PU	0.410	4.47E-15	28.15	0.996	5.65E-6	35.05

a difficulty to do it precisely. Therefore, three steps are used to determine the material constants as follows:

- (i) Firstly, to determine the G_i from the initial value of the Λ vs time curve.
- (ii) Secondly, two steady-stage of the creep strain curves are used to determine the v_s , then by using the best least-square method to find A_s .
- (iii) Finally, subtract the value of $\sigma/G_t + A_s t \sinh(v_s \sigma)$ from $\Lambda(t)$, then use the best least-square method to find G_t, A_t , and v_t .

All these six material constants determined through the above procedures are tabulated in Table I.

To prove the universality of this NFEB model, the stress relaxation tests are conducted in next section.

6. Stress relaxation

Stress relaxation test is conducted by fixing the specimen under constant strain condition and measuring the stress decay with time. a stress-relaxation-test machine (same as the creep testing machine, the only difference is the controlling system is used) to do the stress-relaxation tests. Figure 14 shows a stress decay with time curve, and when the strain become too large the specimen will break. Here we can apply the NFEB model to the stress-relaxation test as follows:

$$\Lambda = \Lambda_i + \Lambda_s + \Lambda_t = \text{constant}$$

$$\sigma = G_t \Lambda_t$$

$$\dot{\Lambda}_s = A_s \text{Sinh}(v_s \sigma)$$

$$\dot{\Lambda}_t = A_t \text{Sinh}(v_t G_t \Lambda_t)$$

Then six material constants determined from the creep test into the above equations to obtain the stress-relaxation model.

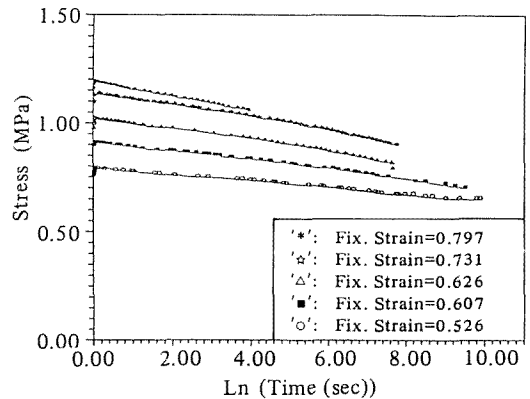


Figure14. Stress dependence of the stress relaxation curve for the 40% V_t of GFSC, where the solid line is the NGEB model's calculation and the mathematical index is the experimental results.

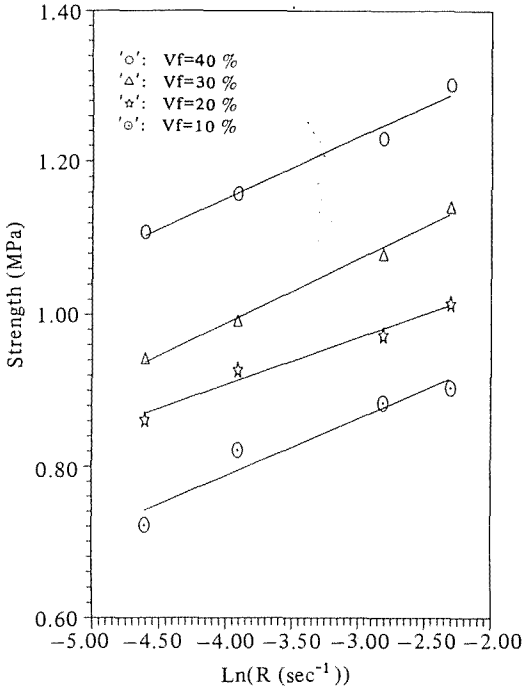


Figure 15. Different V_f of GFSC dependence of the tensile strength vs. strain rate.

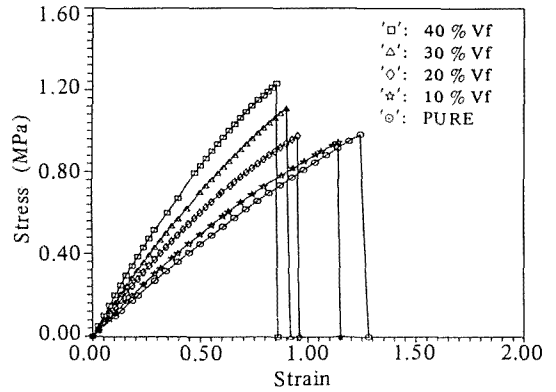


Figure 16. Different V_f of GFSC dependence of the stress-strain curve for the strain rate is 0.06 (1/sec).

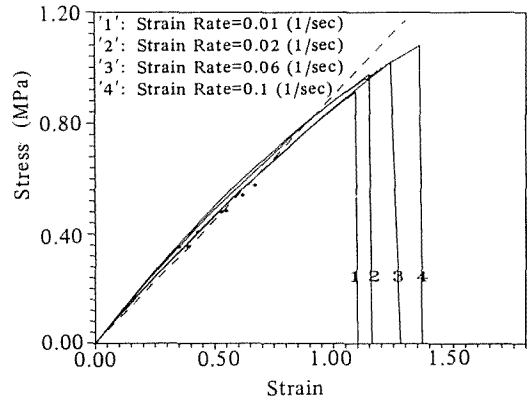


Figure 17. The relation between the initial creep strain Λ_i and the applied stress for the pure silicone rubber, where the solid line is the tensile test results, the dotted line is the rubber elasticity formula calculations and the mathematical index is the creep test results.

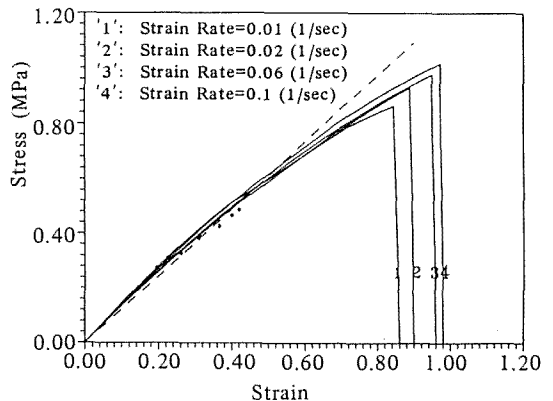


Figure 18. The relation between the initial creep strain Λ_i and the applied stress for the 20% V_f of GFSC, where the solid line is the tensile test results, the dotted line is the rubber elasticity formula calculations and the mathematical index is the creep test results.

Results and Discussion

1. Stress-strain relation

Figures 2-4 show that within the strain-rate range of the creep test there is a negligible strain-rate effect on the stress-strain relation for V_f of GFSC. Besides, the tensile strength is increased as the strain rate increases. Figure 15 shows that the more particles reinforced the more tensile strength GFSC has. It says that the interfacial bonding strength of GFSC is from molecular-chains across the glass-beads, thus, when the material is under stresses the cross-section area due to the Poisson's effect will neck and it induces the tightening of molecular-chain; creating the interfacial friction and providing partial tensile strength. also, Figure 16 shows when the strain rate $R=0.06$ 1/sec, the stress-strain curves of different V_f of GFSC exhibit nonlinear behavior.

2. Creep behavior

Figs 10 and 11 are the creep compliances $C(t) = \epsilon(t)/\sigma$ that vary with time curves of pure silicone rubber and 40% V_f of GFSC respectively. The results show that there is a two-stage variation for the pure silicone rubber. On the other hand, the creep compli-

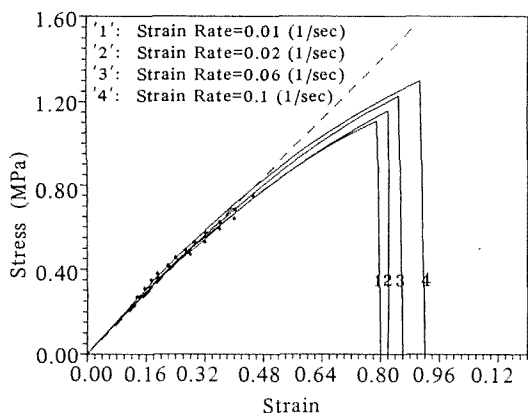


Figure19. The relation between the initial creep strain λ , and the applied stress for the 40% V_f of GFSC, where the solid line is the tensile test results, the dotted line is the rubber elasticity formula calculations and the mathematical index is the creep test results.

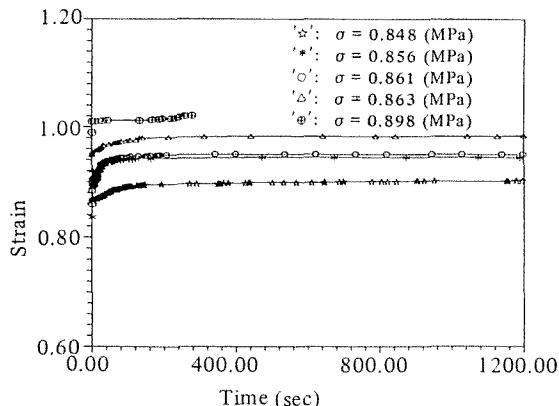


Figure20. Stress dependence of the creep strain vs. time curve for the 20% V_f of the GFSC.

ance of the 40% of GFSC is monotonically increase with increasing time due to the debonding phenomena along the interfaces increasing with time. The results also show that for both materials, the creep compliances increase with increasing stress, and they both exhibit the nonlinear creep behavior relation.

From the uniaxial tensile test, we find that the strain rate effect is limited. Theoretically, the initial creep strain rate should be infinite. Here, we have the initial creep strain values put into the extrapolation of stress-strain curve from the uniaxial tensile test (Figures 17~19) and we find both of them quite consistent. This give us confidence that we can neglect the initial creep strain rate effect. Furthermore, from the dashed line deviated from the stress-strain curve, it says that the rubber elasticity formula is not sufficient to describe the material, especially for the high GFSC which is involved the interface interaction forces. There is a need of another method or model to describe this mechanical behavior.

Figure 20 is the linear creep strain $\epsilon(t)$ vs. creep time curve under different stresses level of the 20% V_f of GFSC. The results show that the curve is shifted upward as the stress is increased. That means the $\epsilon(t)$ increases with increasing loading stress.

3. NFEB model and creep behavior

Figures 6~9 are the typical creep stretch curve of GFSC, where the solid lines are the NGEb model's predictions, and those symbols are the experimental results. They show that the NGEb's model can well describe the GFSC creep behavior-initial stretch, transient-stage stretch and steady-state stretch. and the

creep stretch λ decreases with increasing volume fraction of the GFSC, which is consistent with the physical phenomena.

4. NGEb model and relaxation behavior

If we use the nonlinear mechanical model to describe the relaxation behavior of rubbers, where the material constants are determined from data obtained in creep tests (eg., Table 1), the corresponding relaxation curves can be drawn, and typical results are shown in Figure 14. The model coincides with the experimental results very well for both pure and solid-filled silicone rubbers.

Conclusions

(1) The initial stress-strain curves of the creep test coincide with the stress-strain curves of the uniaxial tensile test. It indicates that the theory of rubber elasticity can well describe the initial stress-strain behavior of the creep test.

(2) Experimental results show that the Eyring's reaction rate principle is suitable to describe the steady stage creep with a constant strain rate. This steady-stage creep occupies the most part of the whole creep history and the material fractures with no symptoms in advance.

(3) The NFEB model based on the entropy spring of the rubber elasticity and the Eyring's reaction-rate principle can well describe the whole creep history of the GFSC. Furthermore, the NFEB model constructed by employing the six material constants determined from the creep test can also predict the stress-relaxation behavior well, which has the tendency of approaching an envelope.

Acknowledgements

The authors wish to express their tanks to Prof. Yih-Hsing Pao for many helpful suggestions. This work is supported by the National Science Council of R.O.C., NSC-80-0405-E002-13.

References

1. L. E. Nielsen, "Mechanical Properties of Polymers and Composites", Marcel Deker, INC. New York (1974).
2. I. M. Ward, "Mechanical Properties of Solid Polymers", 2nd ed., John Wiley & Sons, Ltd. New York (1983).
3. J. J. Aklonis & W.J. Macknight, "Introduction to Polymer Viscoelasticity", 2nd ed., John Wiley & Sons, Inc. New York (1983).
4. W. Flugge, "Viscoelasticity", 2nd revised ed., Springer-Verlag, New York (1975).
5. W. N. Findley, James S. Lai and K. Onaran, "Creep and Relaxation of Nonlinear Viscoelastic Materials-with an Introduction to Linear Viscoelasticity", North-Holland Co., New York (1976).
6. R. M. Christensen, "Theory of Viscoelasticity", Academic Press, Inc. New York (1982).
7. R. S. Rivlin, Rheol. Acta, **22**,160(1983).
8. R. A. Schapery, Polym. Eng. Sci. **9**, 195 (1969).
9. R. M. Christensen, Transactions of ASME, **47**, 762 (1980).
10. L. R. Treloar, "*The Physics of Rubber Elasticity*" (3rd ed.), Oxford Clarendon Press (1975).
11. Y. D. Chen, "*The Creep and Aging Behavior of Solid Particles-Reinforced Hydroxyl Terminated Polybutadiene Rubber Matrix*", Ph.D. Thesis, Institute of Applied Mechanics National Taiwan University, (1990).
12. H. So and Y. D. Chen, Polymer Engineering and Science, March, **31**, No.6, 410-416, (1991).